Current Research in Toxicology 2 (2021) 82–92

Contents lists available at ScienceDirect

Current Research in Toxicology

journal homepage: www.elsevier.com/locate/crtox

Toxicity of poly-dispersed single-walled carbon nanotubes on bone marrow derived Hematopoietic Stem and Progenitor Cells

Md. Babu Mia, Rajiv K. Saxena *

Faculty of Life Sciences and Biotechnology, South Asian University, Akbar Bhawan, Chanakyapuri, New Delhi 110021, India

ARTICLE INFO

Keywords:
Hematopoietic stem cells
Carbon nanotubes
Lymphoid and myeloid differentiation
ROS
Caspase

ABSTRACT

This study has explored the effect of acid-functionalized single-walled carbon nanotubes (AF-SWCNTs) on Hematopoietic Stem and Progenitor Cell (HSPCs) in mouse bone marrow. Administration of AF-SWCNTs induced a significant decline in the live-cell recovery from bone marrow. Lin-negative Stem cell enriched HSPCs internalized AF-SWCNTs that remained localized in cytoplasmic areas. Incubation of HSPCs with AF-SWCNTs resulted in induction of cell death, inhibition of cell cycle, and induction of reactive oxygen species (ROS) as well as the expression of Caspase 3, 7 and 9 enzymes. *In vitro* culture with a cytokine cocktail (SCF, GM-CSF, IL3, IL6, IL7) induced differentiation of HSPCs into lymphocytes and myeloid cells, that was inhibited in presence of AF-SWCNTs. Relative recoveries of lymphocytes specifically B lymphocytes, was significantly reduced by AF-SWCNT-treatment, whereas the relative recovery of myeloid cells remained unaltered. These results suggest that AF-SWCNTs have significant toxic effects on HSPCs and differentially suppress the ontogeny of lymphoid and myeloid cells.

1. Introduction

Hematopoietic activity originating from the Hematopoietic Stem Cells (HSCs) in adult bone marrow is responsible for generating 10^{11}–10^{12} new blood cells per day to replenish the pool of erythrocytes and immune cells (Orkin and Zon, 2008; Wilkinson et al., 2020). Mouse HSCs are characterized by the lack of expression of markers specific for erythrocytes and various kinds of immune cells (lineage negative or Lin^{-}) and expression of Sca1 and cKit markers (LSK) (Yamamoto et al., 2013). Self-renewal and lineage-specific differentiation of HSCs is guided by specific cytokines (Metcalf, 2008). HSCs can differentiate into myeloid progenitor in presence of SCF (Metcalf, 2008; Broudy, 1997), GM-CSF (Metcalf, 2008; Becher et al., 2016) & IL6 (Metcalf, 2008; Bernad et al., 1994; del Carmen Rodríguez, M.a., A. Bernad, and M. Aracil, Interleukin-6 deficiency affects bone marrow stromal precursors, resulting in defective hematopoietic support. Blood, 2004). Lymphoid specific lineages differentiation of HSCs occurs in presence of IL3 (Metcalf, 2008; Xia et al., 1992) & IL 7 (Metcalf, 2008; Akashi et al., 1998; Tani-ichi et al., 2013). Intracellular levels of Reactive Oxygen Species (ROS) play a key role in the physiology of HSCs. ROS^{lo} HSCs efficiently participate in ontogenesis while ROS^{hi} HSCs are prone to proceed towards cell death (Yirong, 2020; Redza-Dutordoir and Averill-Bates, 2016; Shi, 2002).

Carbon nanotubes (CNTs), a man-made isoform of carbon discovered in 1993 (Iijima, 1991) has unique physicochemical properties that make them suitable for wide applications including in electronics and biomedical fields (Chen and Yan, 2017). Acid functionalization of CNT renders them hydrophilic and enhances their interactions with cells while reducing their toxicity *in vivo* (Schipper et al., 2008; Saxena, et al., 2007; Abu Gazia and El-Magd, 2019; Stevens et al., 2006). Carbon nanotube high aspect ratio, nano-dimensions and availability of spare electrons on carbon atoms on its surface that allows chemical coupling with drugs and ligands, make them ideal candidates for drug-targeting *in vivo* (Flores et al., 2020). Results of using carbon nanotubes as a vehicle to deliver drug in BM to treat multiple pathological conditions have seen encouraging (Gangrade and Mandal, 2019; Swami, et al., 2014; Adjei et al., 2016; Jiang et al., 2014). Pristine single-walled carbon nanotubes (SWCNTs) are highly hydrophobic, form huge agglomerates insoluble in aqueous media and therefore do not interact well with biological systems like cells and tis-

Abbreviations: AF-SWCNTs, Acid-functionalized single-walled carbon nanotubes; CNTs, Carbon Nanotubes; FAF-SWCNTs, Fluorescence tagged AF-SWCNTs; HSC, Hematopoietic stem cells; HSPCs, Lineage negative stem cell-enriched cells obtained after negative selection of bone marrow cells; HSPC(dp), $SCA\text{-}1^{+}$ $cKit^{+}$ cell population within HSPCs; ROS, Reactive Oxygen Species.

* Corresponding author.
E-mail addresses: rksaxena@sau.int, rajivksaxena@hotmail.com (R.K. Saxena).

https://doi.org/10.1016/j.crtox.2021.02.003
Received 26 September 2020; Revised 8 February 2021; Accepted 12 February 2021

sues (Saxena, et al., 2007). SWCNTs may be functionalized in a variety of ways to yield hydrophilic poly-dispersed nanotubes that interact well with cells and are therefore used in all biomedical applications (Md and Saxena, 2018; Sachar and Saxena, 2011; Ma et al., 2017; Dutt et al., 2019; Mia and Saxena, 2020; Alam, et al., 2013; Alam et al., 2016; Singh et al., 2020). Previous reports from our group have shown that the acid-functionalized single-walled carbon nanotubes (AF-SWCNTs) may modulate bone marrow and spleen erythropoiesis (Md and Saxena, 2018; Sachar and Saxena, 2011; Ma et al., 2017), suppress T cell and NK cell activation (Mia and Saxena, 2020; Alam, et al., 2013; Alam et al., 2016), interfere with the antigen processing and presentation, and alter epithelial tight junctions(Singh et al., 2020; Rizvi et al., 2015; Kumari et al., 2012). Interestingly, activated T and B lymphocytes internalize significantly higher amounts of AF-SWCNTs and hence their use in down regulating immune disorders like the graft vs host disease have been suggested (Mia and Saxena, 2020).

Use of drug-tagged CNTs for therapeutic purposes would result in a general exposure of the tissues and organs of the recipients and it is important to assess the possible side effects of the CNTs on various organs. Since bone marrow is the source of all blood cells, any damage to bone marrow as a side effect of therapeutic use of CNTs, is of special interest. There is however little information in literature about the interaction of carbon nanotubes with Hematopoietic Stem and Progenitor Cells (HSPCs) and modulatory effect on immune cell ontogenesis. In the present study, we have investigated the interaction and modulatory effect of acid-functionalized single-walled carbon nanotubes (AF-SWCNTs) on enriched populations of HSPCs derived from mouse bone marrow, their self-renewal and the process of ontogenesis yielding immune cells of different types. We found that the *in vivo* administration of AF-SWCNTs induced significant decline in total cell recovery and as well as the recovery of HSPCs from mouse bone marrow. *In vitro*, AF-SWCNTs were quickly internalized by the enriched HSPCs from bone marrow that resulted in suppression of cell proliferation and a cytotoxic response. AF-SWCNT-treatment resulted in a marked up-regulation of levels of ROS as well as the expression of Caspase 3, 7 and 9 enzymes. Culture of HSPCs with a cocktail of crucial cytokines induced proliferation and differentiation of stem progenitors into immune cells that was partially suppressed in presence of AF-SWCNTs. Inhibitory effect of AF-SWCNTs was not uniform across all types of immune cells and the generation of B cells was affected the most.

2. Methods and materials

2.1. Animals

Female C57BL/6N inbred mice (8–12 weeks, 20–25 g body weight) bred under SPF conditions were obtained from Hylasco Biotechnology, Hyderabad and used throughout this study. Animals were housed in the South Asian University animal house facility in positive pressure air-conditioned units (25 °C, 50% relative humidity) and kept on a 12 h light/dark cycle. Water and food were provided *ad libitum*. CO_2-asphyxiation was used as the means of euthanasia. All experimental protocols were duly approved by the University Institutional Animal Ethics Committee (approval code SAU/IAEC/2016/02) and conducted strictly in compliance with the guidelines notified by the Committee for Control and Supervision on Experiments on Animals, Ministry of Environment and Forest (www.envfor.nic.in/divisions/awd/cpcsea_laboratory.pdf).

2.2. Reagents and other supplies

Single-walled carbon nanotubes, 1-ethyl-3-(3-dimethylaminopropyl) carbodiimide (EDAC), N-hydroxysuccinimide (NHS), 2-(N-morpholino) ethane-sulfonic acid (MES) were procured from Sigma Aldrich (St. Louis, MO). 100 kDa dialysis tube and 3 kDa Centricon centrifugal filter device were purchased from Millipore (Billerica, MA). Alexafluor 633 hydrazide was from Molecular Probes (Carlsbad, CA). RPMI-1640 medium (with 2 mM glutamine, 1 mM sodium pyruvate, 4.5 g glucose/L, 10 mM HEPES, 1.5 g/L sodium bicarbonate and 20 μg/mL gentamycin) and fetal bovine serum (FBS) were purchased from Gibco (Carlsbad, CA). Purified anti-mouse CD16/32, fluorochrome tagged anti-mouse Sca1, anti-mouse cKit, anti-mouse CD3, anti-mouse CD19, anti-mouse F4/80, anti-mouse Ly6G/6C antibodies, Annexin V and 7AAD were purchased from Biolegend (San Diego, CA). Ribonuclease A (RNase A), Propidium iodide and CM-H2DCFDA were from Invitrogen (Carlsbad, CA). Caspase-3/7 Green Detection Reagent was purchased from Thermofisher (USA). Mouse hematopoietic stem and progenitor stem cells (HSPC) isolation negative enrichment kit Mojosort were purchased from Biolegend (San Diego, CA). StemSpan Serum-Free Expansion Medium (SFEM) (containing IMDM, Bovine serum albumin, Recombinant human insulin, Human transferrin (iron-saturated), 2-Mercaptoethanol Supplements) and cytokines (mouse recombinant SCF, GM-CSF, IL3, IL6, IL7) were procured from Stemcell technologies (Vancouver, Canada). DAPI was purchased from Sigma Aldrich (USA). SYBR-iTAQ Universal SYBR Green super mix was purchased from Bio-Rad Laboratories (California, USA). cDNA Synthesis kit and RNA Iso-Plus Trizol were purchased from DSS TaKara (India).

2.3. Acid functionalization of SWCNTs

Acid-functionalized Single-walled carbon nanotubes (AF-SWCNTs) were prepared as described before (Sachar and Saxena, 2011). Briefly, SWCNTs (Sigma, Cat# 775535, > 95% carbon) (20 mg) were suspended in 20 ml concentrated H_2SO_4 and HNO_3 (1:1) mixture and subjected to high pressure microwave (20 ± 2 psi, 50% of 900 W power, and temperature 135–150 °C) for 3 min. Suspension was cooled, diluted 2X in water, dialyzed against deionized water, and lyophilized for further use. AF-SWCNT preparations thus obtained comprised black powder easily disbursable in aqueous media and had no residual acids in it. AF-SWCNTs were characterized using Malvern DLS Zetasizer. AF-SWCNT particles had an average size of 277.06 ± 3.37 d. nm and an average zeta potential of −47.02 ± 0.69 mV. Flow BET nitrogen adsorption technique indicated a BET surface area 799.399 M_2/g for AF-SWCNT preparation. Transmission electron microscopic (TEM) study (magnification-50000×) of pristine and acid functionalized SWCNTs revealed that the acid functionalization significantly reduced carbon nanotubes agglomeration without disturbing their basic structure (Supplementary Fig. S1). To obtain Fluorescent tagged AF-SWCNTs (FAF-SWCNTs), AF-SWCNTs were covalently tagged with fluorochrome Alexa fluor 633 as described elsewhere (Sachar and Saxena, 2011).

2.4. Isolation of Hematopoietic stem and Progenitor cells (HSPCs) from bone marrow cells

Mice were euthanized using carbon dioxide and bone marrow cells collected from their tibia and femur bones. HSPCs were isolated by using the negative selection magnetic sorting kit (Mojosort) using the protocol suggested by the manufacturers. Briefly, bone marrow cells (10×10^6 in 100 μl of PBS) were incubated with 10 μl of biotinylated antibody cocktail (anti-CD3ε, CD45R/B220, Ly-6G/Ly-6C (Gr-1), CD11b, TER-119 antibodies) for 20 min in ice. Streptavidin Nanobeads were added to the suspension followed by incubation for 20 min. Cells were washed with PBS and the pelleted cells were suspended in 2.5 ml PBS. Cell suspension in 5 ml plastic tube was placed in EasySep Magnet for 5 min. HSPCs suspension was gently decanted into a fresh tube. Magnetic separation was repeated once.

2.5. Uptake of FAF-SWCNTs by HSPCs

HSPCs (1×10^6) were incubated with FAF-SWCNTs (20 μg per ml of RPMI complete medium per well) in 48 well plate. Cells were harvested at 4 h and stained with fluorochrome tagged anti-mouse Sca1 and cKit antibodies. Uptake of FAF-SWCNTs by different subsets of HSPCs was analyzed by flow cytometry.

2.6. Flow cytometric assay

Cells to be analyzed were incubated with Fc block (anti-mouse CD 16/32, 0.5 μg/10^6 cells in 100 μl of PBS containing 2% FBS) for 30 min in ice. Cells were then stained with the required fluorochrome tagged antibodies or the respective isotype control antibodies as described before (Dutt et al., 2019). Briefly, cellular debris in the cell samples was excluded on FSC vs SSC histograms. Cells stained with isotype control antibodies were used to set gates for detection of cells stained with specific phenotyping antibodies. Due care was used for color compensation to avoid spill-over of cellular populations.

Propidium iodide (PI) staining and cell cycle study was carried out as described before (Dutt et al., 2019). Briefly, cells with or without specific antibody stain were fixed overnight using 70% ethanol at 4 °C in the dark followed by treatment with Ribonuclease A (50 μg/mL, 2 h at 37 °C) and PI staining (5 μg/ml PI, 30 min in ice). Flow cytometric analysis was performed using FACSuite, FlowJo v10 and Modfit v3.1 softwares.

2.7. Confocal microscopy

To study the uptake and localization of FAF-SWCNTs, HSPCs (1×10^6) were incubated with FAF-SWCNTs (20 μg/ml of RPMI complete medium) in 48 well-plate. Cells were harvested at 4 h and stained with anti-mouse Sca1 and cKit antibodies. $Sca1^+cKit^+FAF\text{-}SWCNT^+$ cells were isolated by cell-sorting using FACSAria III cell sorter, fixed in 2% paraformaldehyde. Fixed cells were washed, and adhered onto poly-L-lysine coated coverslip and stained with DAPI (100 ng/ml) as described before (Dutt et al., 2019). Excess stain was removed by washing coverslips with cells with PBS. Coverslips were air-dried, mounted on glass slides using prolong gold anti-fade reagent, and analyzed using A1R Laser Confocal Scanning Microscope (Nikon, Japan) at 100X magnification.

2.8. Differentiation of HSPCs by culturing with cocktail of cytokine

HSPCs (0.1×10^6) were cultured in SFEM media containing cytokine cocktail (SCF, GM-CSF, IL3, IL6, IL7, 33 ng/ml final concentrations of each cytokine) with or without AF-SWCNTs (50 μg/ml) in 24 well culture plates (1 ml /well). On the 5th day, 700 μl media was removed from the wells without disturbing the cells and replaced with equal volume of fresh SFEM media with cytokine cocktail. On the 8th day, cells were harvested and counted using a hemocytometer. Cells were stained with anti-mouse Sca1, cKit, CD3, CD19, F4/80, Ly6G/6C antibodies, and analyzed using flow cytometry.

2.9. Estimation of reactive oxygen species (ROS) and Caspase 3/7 in HSPCs

Estimation of reactive oxygen species (ROS) in control and AF-SWCNT-treated HSPCs was done by using the CM-H_2DCFDA dye as described elsewhere (Oparka et al., 2016). ROS detection reagent (CM-H_2DCFDA, 10 μM) was added to cell cultures, cells harvested after 1 h and analyzed using FACSVerse and examined under a fluorescence microscope. Expression of caspase 3 and 7 enzymes in control and AF-SWCNT-treated HSPCs was examined by using the Caspase 3/7 detection kits as described before (Huang et al., 2011). Briefly, HSPCs (0.3×10^6) were incubated with or without AF-SWCNTs (50 μg/ml) per ml of RPMI complete media per well of 24 well-plate. Caspase-3/7 green detection reagent (7.5 μM) was added to cells suspension at the beginning of the culture, cells harvested at 24 h and analyzed on FACSVerse using Flowjo software and also under a fluorescence microscope.

2.10. RT-PCR analysis

RT-PCR technique was used to assess the expression levels of mRNA as described before (Nolan et al., 2006). Briefly, HSPCs (2×10^6) were incubated without/with AF-SWCNTs (100 μg/ml, 1 ml suspension per well of 48 well culture plates) in RPMI complete media. Cells were harvested after 24 h and incubated with Trizol reagent to extract total RNA. cDNA was synthesized with a cDNA synthesis kit using 2 μg total RNA. Forward and Reverse sequences of primers were as follows:

β-actin: Forward primer: GGAGGGGGTTGAGGTGTT
Reverse primer: GTGTGCACTTTTATTGGTCTCAA
Caspase-9: Forward primer: GAGGAGAGTGTGGAATCTG
Reverse primer: TACCAAGAGGTGGAACGACA
Caspase-3: Forward primer: ATGGACTAACACGAGCGTAG
Reverse primer: GACGATCTGAGGGTACAGATT

Total reaction volume was 10 μl (consisting 2.5 μl of ten-fold diluted cDNA, 5 μl SYBR green, 0.2 μl of each primer (10 mM), 2.3 μl sterile distilled water). Cycling condition was 10 min at 95C, 40 cycles of 15 sec at 95C, 30 sec at 60C and the melt curve with single reaction cycle was 95C for 15 sec, 60C for 1 min and dissociation at 95C for 15 sec. The cycle threshold (Ct) values were obtained after amplification from Real time PCR-ViiA 7 machine and normalized to the value of housekeeping β-actin gene. 2-ΔΔCt method were used to calculate target genes relative expression.

2.11. Statistical analysis

Each experiment was repeated three times with minimum three mice in each group. Data analysis was performed using Sigma Plot software (Systat Software, San Jose, CA). Results were presented as Mean ± SEM. Statistical significance between groups were calculated using student's *t*-test or ANOVA. *P* value < 0.05 was accounted as significant ($P \leq 0.05$ *, < 0.01 **, < 0.005 ***, < 0.001 ****).

3. Results

3.1. Effect of administration of AF-SWCNTs on mouse bone marrow

Effect of *in vivo* administration of AF-SWCNTs in mice was examined on the recovery of bone marrow cells and stem cells. A survey of literature indicates that for studying the toxicity *in vivo* in mouse model, a wide range of intravenous doses (2–40 mg/kg) have been used as there is no apparent acute toxicity in this dose range (Liu et al., 2009; Zhang et al., 2020; Wu et al., 2009). As in our previous studies (Alam, et al., 2013; Alam et al., 2016), we used an *i.v.* dose of 100 μg/mouse AF-SWCNTs that corresponded to a 5 mg/kg dose. Two doses of 100 μg each in 100 μl PBS at 0 h and 24 h, or PBS alone were administered intravenously in mice. At 48 h time point, bone marrow cells were harvested and live bone marrow cells (trypan blue negative) counted using hemocytometer. Fig. 1A shows, AF-SWCNTs treatment reduced the recovery of bone marrow cells per mouse by about 36%. Bone marrow cell preparations harvested from control and AF-SWCNT-treated mice were also stained with Sca1 and cKit antibodies to enumerate single positive, double positive and double negative cells by flow cytometry. Mean absolute recovery of HSPCs (expressing cKit or SCA-1 markers or both), from bone marrow however declined by 48% in AF-SWCNT-treated mouse (Fig. 1B), suggest-

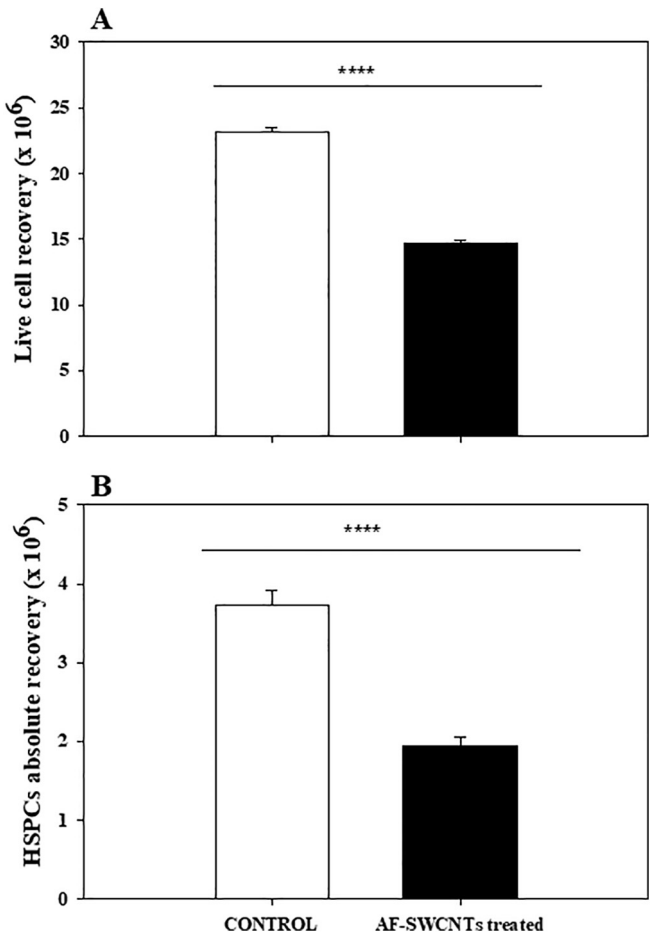

Fig. 1. *In vivo* cytotoxicity of AF-SWCNTs on mouse bone marrow. C57Bl/6N Mice were administrated intravenously PBS (100 μl/mouse) or AF-SWCNTs (100 μg/mouse in 100 μl PBS) at 0 & 24 h. Mice were sacrificed 24 h after the last injection and BM cells harvested. Total recovery of live bone marrow cell was assessed by hemocytometer counting using Trypan Blue vital dye. Cells were stained with Sca1 and cKit antibodies and analyzed by flow cytometry. Panel A represents mean total recoveries of live bone marrow cells from control and AF-SWCNT-treated mice. Panel B shows absolute recoveries of HSPCs that were positive for Sca1 and/or cKit, (excluding double negative cells) in bone marrow cells isolated from control and AF-SWCNT-treated mice. Data represents Mean ± SEM. Statistical significance between groups were calculated using student's *t*-test or ANOVA ($p < 0.001$ ****, n = 6 mice).

ing that HSPCs could be more susceptible to the toxic effect of AF-SWCNTs. The difference between the 36% and 48% declines in the two groups though small was nonetheless statistically significant ($p < 0.001$).

3.2. Enrichment of bone marrow HSPCs by negative selection and uptake of FAF-SWCNTs

Above results suggest that the administration of AF-SWCNTs may have a significant suppressive effect on bone marrow in mice. Bone marrow comprises a complex tissue with high cell proliferation and differentiation activities as well as cellular flux as different types of cells regularly move in and out of bone marrow. In order to understand the modulatory effect of AF-SWCNTs on HSPCs, we used the *in vitro* culture system where cytokine driven cell division and differentiation of stem cells and progenitor cells could be examined in isolation.

Stem cells from mouse bone marrow were enriched by negative selection process as described in Methods. Bone marrow cells thus enriched by negative selection will be referred to as HSPCs (Hematopoietic Stem and Progenitor cells). HSPCs were stained with Sca1 and cKit antibodies. Staining patterns of control bone marrow cells and that of HSPCs in Fig. 2A show that the negative selection resulted in an enrichment of $Sca1^+$ cells from 4.72% to 14.75%, $cKit^+$ cells from 16% to 38.9% and double positive cells from 2.43% to 10.3% (Fig. 2A).

In order to assess the uptake of nanotubes, HSPCs were incubated with fluorescence tagged AF-SWCNTs (FAF-SWCNTs) for 4 h. Flow cytometric results in the left panel of Fig. 2B show that all HSPCs were positive for FAF-SWCNT uptake. We also found 100% uptake of FAF-SWCNTs even in unfractionated control bone marrow cells (results not shown). Further analysis of FAF-SWCNT uptake by different subsets of HSPCs was examined by first incubating the cells with FAF-SWCNTs, followed by staining with SCA-1 and cKit antibodies and examination by flow cytometry. Flow cytometry results are shown in flow-histogram in Fig. 2B (right panel). Mean fluorescence intensity of FAF-SWCNT stain (a measure of average FAF-SWCNT uptake per cell) in each quadrangle is given in the data table in Fig. 2B. These results show that even though cells in all four quadrangles were positive for FAF-SWCNT uptake, maximum relative uptake was in $Sca1^+$ cells in quadrangle A. cKit positive and double positive cells in quadrangles C and B respectively, had relatively lower uptake of FAF-SWCNTs.

Uptake of FAF-SWCNTs by $Lin^-Sca1^+cKit^+$ cells [HSPCs double positive for SCA-1 and cKit markers termed HSPC(dp)] was further examined by confocal microscopy. For this purpose, HSPCs were incubated with FAF-SWCNTs and stained with SCA-1 and cKit antibodies. HSPC(dp) cell preparations were isolated by cell sorting on a FACSAria III cell sorter, and examined for FAF-SWCNT uptake using a confocal microscope as described in Methods. Results in Fig. 2C (upper panel) show that all HSPC(dp) cells had internalized FAF-SWCNTs (red fluorescence). The fluorescent particles were more prominent in the cytoplasmic areas and much less so in the nuclear area. Lower panel of Fig. 2C shows the Z-sectioning data at several depths that indicate the particles were truly inside the cells and not attached to the cell membranes.

3.3. AF-SWCNTs cytotoxicity on HSPCs

Induction of cytotoxicity in response to AF-SWCNTs was examined in HSPCs by incubating these cells with AF-SWCNTs (50 μg/ml) for 24 h followed by staining with Annexin-V and 7AAD to assess apoptotic and necrotic responses. Recovery of live cells at the end of 24 h incubation was reduced by about 40%. Proportion of Annexin-V stained cells (Apoptotic cells) did not rise in AF-SWCNT-treated cells (Fig. 3A and left panel of Fig. 3B) but 7AAD positive cells increased from 14.35% (control cells) to 25.7% in AF-SWCNTs treated cells. Cell cycle analysis of the control and AF-SWCNT treated cells was carried out to assess the changes in cell cycling pattern. Results in Fig. 3B right panel show that the percentages of cells in G0/G1, S, G2/M phages in control HSPCs were 71.93%, 27.84%, 0.23% respectively for and 80.74%, 19.25%, 0.00% respectively in AF-SWCNTs treated HSPCs. Taken together, our results suggest that AF-SWCNTs exerted significant cellular toxicity as well as stagnation of the cell cycle.

3.4. Reactive oxygen species (ROS) and Caspase 3/7 responses in HSPCs

To further investigate the molecular mechanism of AF-SWCNT induced cell death, HSPCs were incubated with CM-H_2DCFDA dye in presence or absence of AF-SWCNTs for one hour and fluorescent signals generated due to ROS response was assessed by flow cytometry. Relative Mean fluorescence intensity (MFI) due to intercellular ROS increased from 3452 to 16,030 upon AF-SWCNTs treatment (Fig. 4A top panel). Immunofluorescence microscopy data (Fig. 4A bottom two panels) confirmed the flow cytometry data and shows that control cells had a baseline ROS generation that increased markedly in AF-

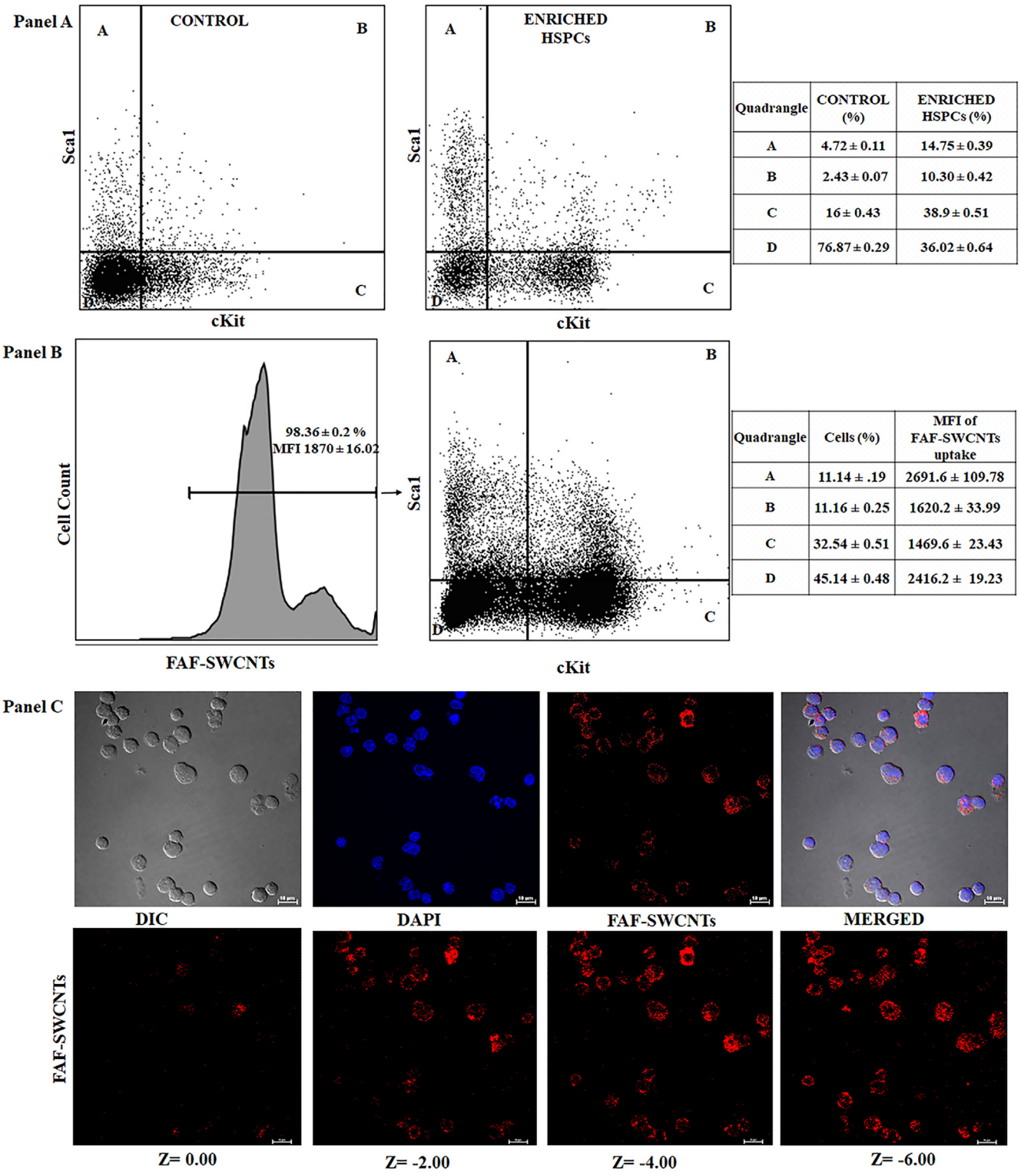

Quadrangle	CONTROL (%)	ENRICHED HSPCs (%)
A	4.72 ± 0.11	14.75 ± 0.39
B	2.43 ± 0.07	10.30 ± 0.42
C	16 ± 0.43	38.9 ± 0.51
D	76.87 ± 0.29	36.02 ± 0.64

Quadrangle	Cells (%)	MFI of FAF-SWCNTs uptake
A	11.14 ± .19	2691.6 ± 109.78
B	11.16 ± 0.25	1620.2 ± 33.99
C	32.54 ± 0.51	1469.6 ± 23.43
D	45.14 ± 0.48	2416.2 ± 19.23

Fig. 2. Enrichment of HSPCs by negative selection and the uptake of FAF-SWCNTs by HPSC(dp). Results in panel A show the distribution of Sca1 and cKit markers on fresh bone marrow cells and HSPCs obtained by negative selection process. HSPCs were incubated with fluorescence tagged AF-SWCNTs (FAF-SWCNTs, 20 μg/ml of RPMI complete medium per well for 4 h), washed, counter stained with Sca1 and cKit antibodies and analyzed for FAF-SWCNTs by $Sca1^{+}cKit^{+}$, $Sca1^{+}cKit^{-}$, $Sca1^{-}cKit^{+}$, $Sca1^{-}cKit^{-}$, cell populations. Results in panel B (left panel) show that all 100% of the cells were positive for FAF-SWCNT uptake. Right panel shows the 2D flow histogram dividing the cells on the basis of Sca1 and cKit expression, and mean channel fluorescence (MFI) of FAF-SWCNT uptake in all four subpopulations. Quantitative data of quadrangle populations and their FAF-SWCNT-uptake is given in the table in panel B. Panel C shows the confocal data on uptake of FAF-SWCNTs in $Sca1^{+}cKit^{+}$ double positive HSPCs [HSPC(dp)]. Quadrangle B cells from Panel B were isolated by using FACSAria III cell sorter and processed for confocal microscopic examination as described in Methods. Upper panel shows the uptake of FAF-SWCNTs and the lower panel shows Z-sectioning of cells to demonstrate intracellular localization of FAF-SWCNTs. n = 6 mice were used throughout the experiment.

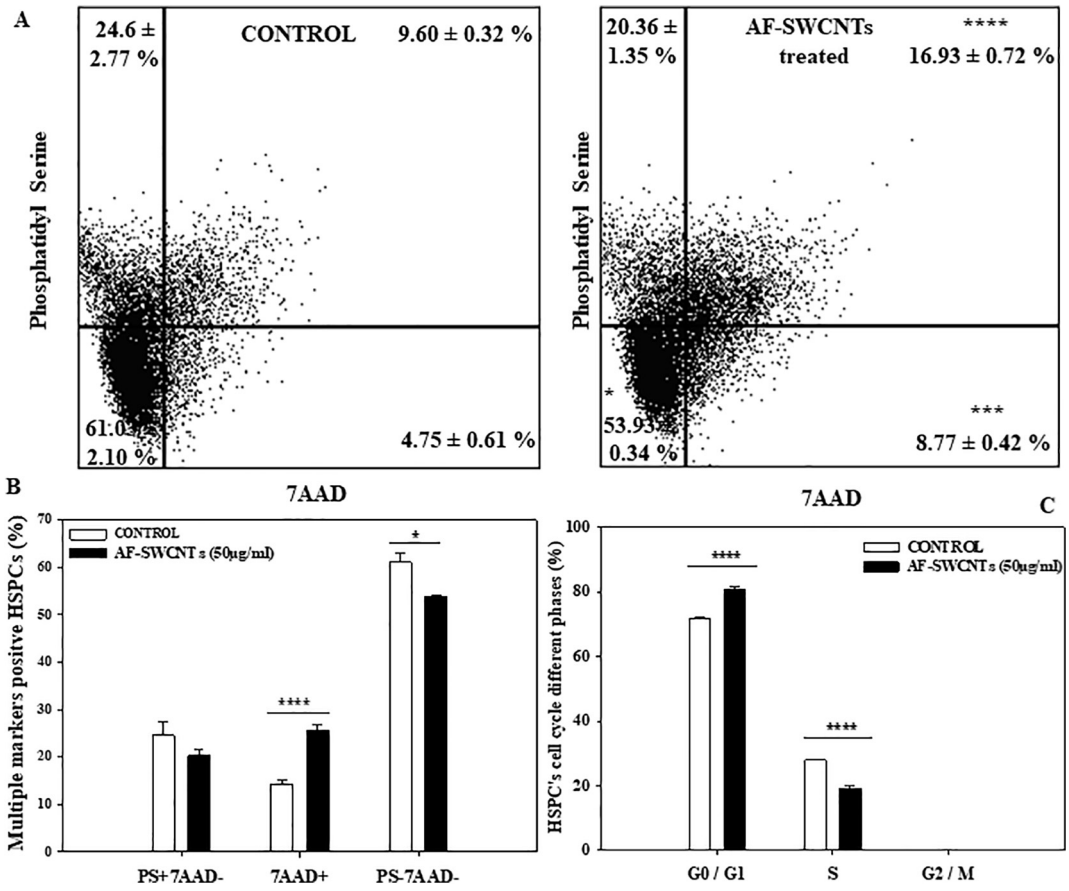

Fig. 3. AF-SWCNTs cytotoxic effect on HSPCs in 24 h. HSPCs (1×10^6 cells/ml complete RPMI medium) were incubated with or without AF-SWCNTs (50 µg/ml) for 24 h. Cells were stained with Annexin V and 7AAD as described in Methods. Panel-A shows the data on Phosphatidyl Serine (PS) and 7AAD staining patterns of control and AF-SWCNT-treated cells. Panel B shows the comparison of proportions of PS + 7AAD-, PS + 7AAD + and PS-7AAD + in control and AF-SWCNT-treated cells. Control and AF-SWCNT treated cells were also analyzed for cell cycle by propidium iodide staining protocol as described in Methods. Data in Panel-C shows the comparisons of proportions of cells in G0/G1, S and G2/M phases of cell cycle in control and AF-SWCNT-treated cells. Data represents Mean ± SEM. Statistical significance between groups were calculated using student's *t*-test or ANOVA. ($p < 0.05$ *, < 0.01 **, < 0.005 ***, < 0.001 ****). n = 6 mice were used throughout the experiment.

SWCNT treated cells. Similar data for Caspase 3/7 enzyme activity is provided in Fig. 4B where the activation was examined after 24 h incubation of the HSPCs with AF-SWCNTs. Thus, the treatment with AF-SWCNTs induced marked activation of both ROS and Caspase 3/7 enzymes in HSPCs.

3.5. Upregulation of ROS and Caspase 3/7 genes in HSPCs by AF-SWCNTs treatment

Results above show that AF-SWCNTs induced cytotoxicity in HSPCs could be mediated through the ROS and Caspase 3/7 activation pathways. Generation of ROS and Caspase enzymes would require activation of their respective genes. Activation of ROS and Caspase genes was examined by RT-PCR technique. RT-PCR was carried out as described in Methods and fold change in gene expression was calculated using $2 - \Delta\Delta Ct$ method, normalized with the expression of house-keeping β-actin gene. Results in Fig. 5 show that the AF-SWCNT treatment augmented significantly the expression of Caspase-9 (↑17.82, $P < 0.01$) and Caspase-3 (↑125.10, $P < 0.01$) genes (Fig. 5).

3.6. Modulation of stem-cell ontogenesis in vitro by AF-SWCNTs

HPSCs may be induced to differentiate to a variety of immune cells *in vitro* if cultured with a cocktail of cytokines that aid the proliferation and differentiation process (Metcalf, 2008; Broudy, 1997; Becher et al., 2016; Bernad et al., 1994; del Carmen Rodríguez, M.a., A. Bernad, and M. Aracil, Interleukin-6 deficiency affects bone marrow stromal precursors, resulting in defective hematopoietic support. Blood, 2004; Xia et al., 1992; Akashi et al., 1998; Tani-ichi et al., 2013). HSPCs (0.1 million cells in 1 ml medium per culture well) were cultured with cytokine cocktail (SCF, GM-CSF, IL3, IL6, IL7) with or without AF-SWCNTs (50 µg/ml) as described in Methods. Cells were harvested at 8th day. Total mean live cell recovery in control cultures was 0.25 ± 0.097 million cells per well that indicated about 2.5-fold increase in cell numbers per well. In AF-SWCNT treated cultures, the average recovery of live cells was 0.0966 ± 0.0027 million cells that represented no increase in cell numbers. Overall, there was a 60% fall in live cell recovery in AF-SWCNT-treated cultures.

Cells recovered from cultures were stained for Sca1, cKit, CD3, CD19, F4/80 and Ly6G/6C markers and examined by flow cytometry to assess the proportions of different types of stem cells and immune cells at the end of 8 days culture. It should be noted that in the beginning of the culture of HSPCs, there were no cells that expressed the CD3, CD19, F4/80 and Ly6G/6C markers. Culturing with the cytokine cocktail resulted in the generation of different types of immune cells. Proportions of $CD3^+$ T-cells, $CD19^+$ B-cells, $F4/80^+$ macrophages/-monocytes, Ly6G/6C expressing myeloid cells as well as $Sca1^+$ and/or $cKit^+$ cells in control and AF-SWCNT-treated cultures are shown in Fig. 6A. These results show that a significant proportion of cell

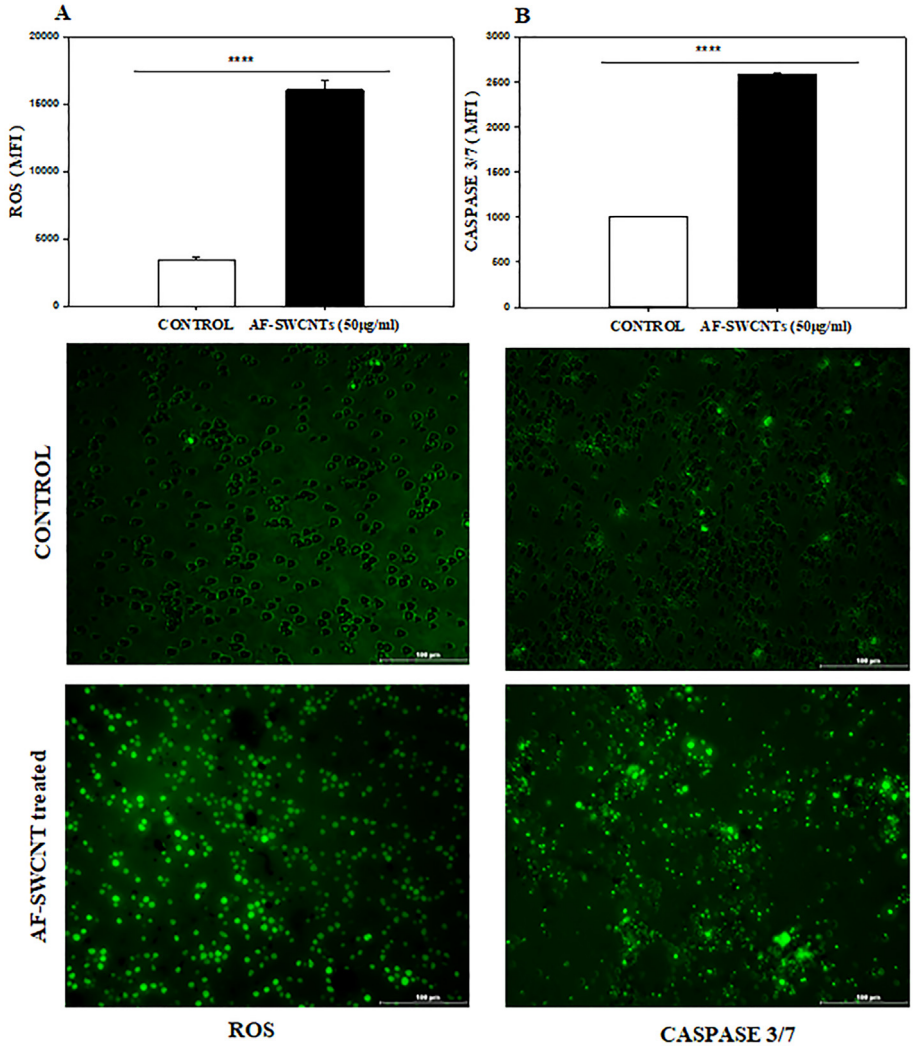

Fig. 4. Expression of ROS and Caspase 3/7 on control and AF-SWCNT-treated HSPCs. HSPCs (1×10^6 cells/ml complete RPMI medium) were incubated with or without AF-SWCNTs (50 µg/ml) for 1 h (ROS expression) or 24 h (Caspase 3/7 expression). Fluorescence generating assays for ROS and Caspase detection were carried out as described in Methods. Panel A shows the flow cytometric data on the ROS and Caspase signals generated in control and AF-SWCNT-treated cells. Panel B shows the intensities of ROS and Caspase signals as reveled by confocal microscopy. Data in panel A represents Mean ± SEM. Statistical significance between groups were calculated using student's *t*-test or ANOVA. ($p < 0.001$ ****). n = 9 mice were used throughout the experiment.

recovered from control as well as AF-SWCNT-treated cultures were differentiated immune Cells. However relative proportions of these cells differed in control and AF-SWCNT-treated cultures. A significant decline was seen in the proportions of SCA-1 and/or cKit positive HSPCs (23%), B cells (38%) and macrophages (10%) in AF-SWCNT-treated cultures whereas a small yet significant increase was seen in the proportions of T cells and Myeloid cells (Fig. 6A). Setting of flow cytometric gates for collecting this data has been illustrated in Supplementary Fig. 2.

Fig. 6B shows the absolute recoveries of different cell types in control and AF-SWCNT-treated cultures of HSPCs. Absolute cell recoveries were markedly lower for all cell populations. This was expected since the overall recovery of live cells was 60% lower in AF-SWCNT-treated cultures.

These results indicate that HSPCs cultured with cytokine cocktail not only reproduced themselves, but also divide and differentiate into a variety of immune cells that represents ontogenesis *in vitro*. This ontogenesis occurs in presence of AF-SWCNTs also but the cell recovery is markedly lower by about 60%. AF-SWCNTs thus appear to be toxic to both HSPCs as well as the newly formed immune cells. Yet the suppression of division and differentiation processes is not uniform across all cell types. Generation of B-cells and macrophages is more prone to suppression as compared to T cells and myeloid lineage cells. A comparison of relative proportions of HSPCs, lymphoid and myeloid cells in HSPCs before and after culture with cytokine cocktail in presence and absence of AF-SWCNTs is shown in form of pie charts in Fig. 7. Proportion of stem cells declined from 64% in fresh HSPCs to 28% in control cultures with cytokine cocktail and to 21.5% in cultures where both cytokines and AF-SWCNTs were added. The fall in proportion of stem cells from freshly isolated enriched cells to the cells cultured with cytokines for 8 days does not represent an actual fall in absolute number of stem cells as the cell recovery itself went up 2.5-fold in cytokine treated cultures. A significant fall in the proportion of lymphoid cells (combined $CD19^+$ B cells and $CD3^+$ T cells) from 25.8% in control cultures to 18.6% in AF-SWCNT-treated cultures) was observed indicating that the generation of lymphoid cells was relatively more affected in AF-SWCNT-treated cultures. Proportion of myeloid cells (combined F4/80 + macrophages and Ly6G/6C + myeloid cells) did not change significantly in AF-SWCNT-treated cultures. These results clearly indicate that cell divi-

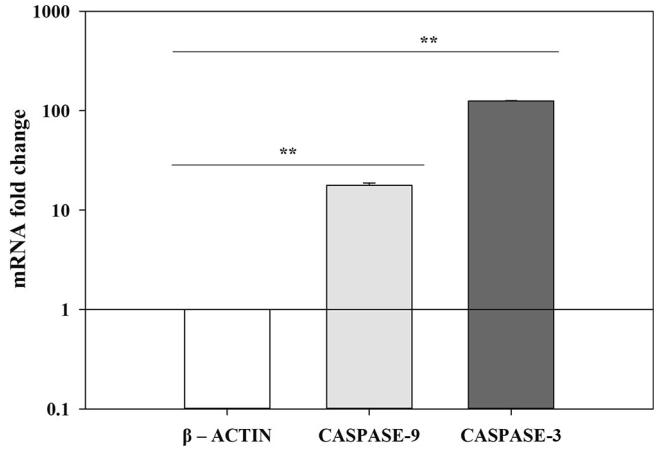

Fig. 5. RT-PCR analysis of expression of Caspase 3 and Caspase 9 genes in control and AF-SWCNT-treated HSPCs. HSPCs (1×10^6 cells/ml complete RPMI medium) were incubated with or without AF-SWCNTs (100 μg/ml) for 24 h. RNA was extracted and RT-PCR analysis carried out as described in Methods. Bar graphs represent fold changes in mRNA of Caspase 9 and Caspase 3 genes. Data represents Mean ± SEM. Statistical significance between groups were calculated using student's *t*-test or ANOVA. ($p < 0.01$ **). n = 12 mice were used throughout the experiment.

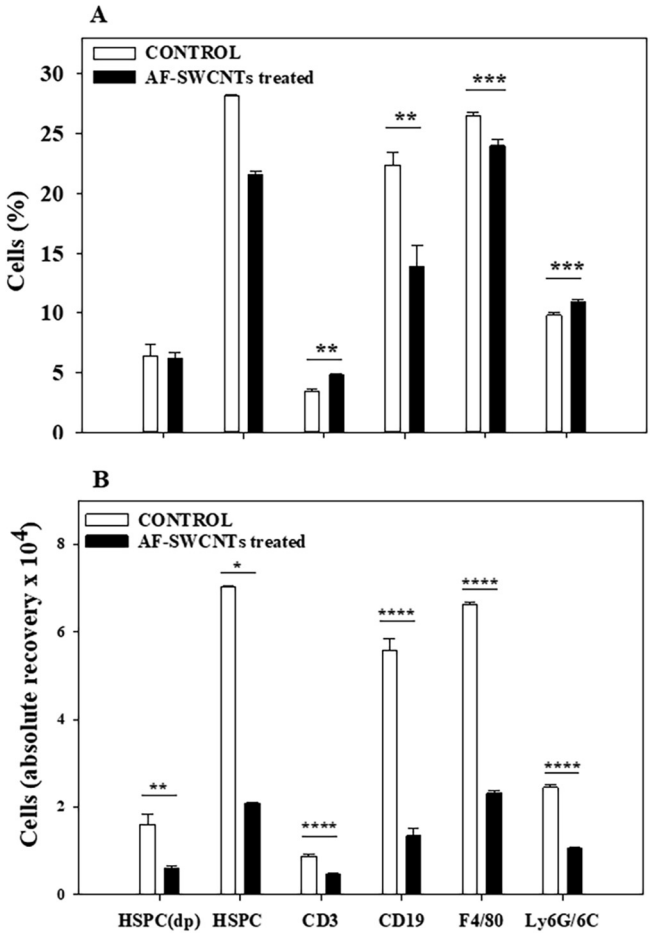

Fig. 6. Cytokine-driven self-renewal and differentiation of HSPCs into lymphoid and myeloid cells in presence or absence of AF-SWCNTs. HSPCs (0.1×10^6/ml per well) were incubated with cytokine cocktail (SCF, GM-CSF, IL3, IL6, IL7, 33 ng/ml each) in SFEM media with or without AF-SWCNTs (50 μg/ml) for 8 days as described in Methods. Cells were harvested and stained with Sca1, cKit, CD3, CD19, F4/80 and Ly6G/6C antibodies and analyzed on flow cytometer. Panel A compares the proportions of cells expressing different markers in control and AF-SWCNT-treated cultures. Panel B shows their absolute recovery of the same six populations. HSPCs bars in the histogram represent cells expressing SCA-1 and/or cKit markers. All data represents Mean ± SEM. Statistical significance between groups were calculated using student's *t*-test or ANOVA. ($p < 0.05$ *, < 0.01 **, < 0.005 ***, < 0.001 ****). n = 6 mice were used throughout the experiment.

sion and differentiation promoted by cytokines was not completely blocked by AF-SWCNTs but the generation of lymphoid cells was relatively more affected.

4. Discussion

It is important to understand the interactions of carbon nanotubes (CNTs) with biological systems for several reasons. Firstly, their extensive use in a wide spectrum of commercial applications necessitates high volume manufacturing of CNTs. Nature does not have efficient mechanisms to degrade CNTs (Iijima, 1991). Environmental accumulation of CNTs and consequential exposure of life forms would therefore be inevitable. It follows that the biological consequences of such sustained exposure must be understood. Secondly, functionalized CNTs are fast becoming a favorite agent for drug delivery *in vivo* (Prato et al., 2008; Liu, 2011; Canu, 2020) and biological effects of exposure to functionalized CNTs must be understood in order to refine the use of CNTs *in vivo*. In addition, while CNTs at present do not constitute a significant pollutant in the environment, occupational exposures to workers involved in commercial applications of CNTs is possible (Kobayashi et al., 2017). Our research over last couple of decades has focused on the effects of carbon nanoparticles including CNTs on a variety of biological parameters especially the immune system (Saxena, et al., 2007; Stevens et al., 2006; Sachar and Saxena, 2011; Ma et al., 2017; Dutt et al., 2019; Mia and Saxena, 2020; Alam, et al., 2013; Alam et al., 2016; Singh et al., 2020; Rizvi et al., 2015; Kumari et al., 2012). Since the whole of the immune system basically originates in bone marrow, it is pertinent to ask the question as to how CNTs would influence the hematopoietic stem cells and ontogenesis leading to different types of immune cells. A literature survey indicates that not much is known about the interactions of CNTs with bone marrow stem cells and the process of ontogenesis.

The current study is an attempt to gain some insight into the interactions of CNTs with bone marrow. We have used acid-functionalized single-walled-carbon nanotubes (AF-SWCNTs) since this is the form that is stable in aqueous media and interacts efficiently with a variety of cell types (Schipper et al., 2008; Saxena, et al., 2007; Abu Gazia and El-Magd, 2019; Stevens et al., 2006). Acute toxicity of CNTs in mice has been well studied (Kobayashi et al., 2017; Madani et al., 2013; Ahmadi et al., 2017). In general, functionalized carbon nanotubes have a rather short life in blood circulation and are rapidly excreted through kidney and gall bladder (Liu et al., 2008) and do not induce significant acute toxic responses or death in mice (Madani et al., 2013). We used an *i.v.* dose of 100 μg per mouse that is well within the range of doses commonly used in other toxicological studies in mice for CNTs and not associated with acute toxicity in mice (Liu et al., 2009; Zhang et al., 2020; Kobayashi et al., 2017). In our own previous studies, 100 μg dose of AF-SWCNTs induced transient anemia in mice but the mice recovered soon (Sachar and Saxena, 2011). We have also shown the *in vivo* suppression of CTL and NK cell activation by using the same dose of AF-SWCNTs (Alam, et al., 2013; Alam et al., 2016). A similar dose of CNTs was used by Wu et al. for cancer therapy in mice using drug-tagged CNTs (Wu et al., 2009). The doses of AF-SWCNTs we used in our present study *in vitro* or *in vivo* are thus in the same range as have generally been used by us and others.

Our initial experiments clearly show that the administration of AF-SWCNTs resulted in an atrophy of bone marrow in form of reduced

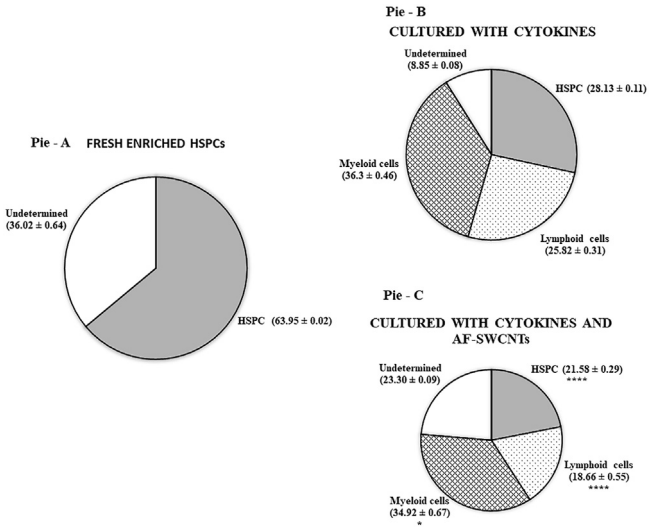

Fig. 7. Comparative Pie charts to show the proportions of stem cells, lymphoid cells and myeloid cells in fresh HSPC-enriched cells, and culturing with cytokine cocktail with or without AF-SWCNTs. Data in Fig. 6 has been represented here for proportions of HSPCs (total of cells positive for Sca1, cKit, and both, excluding double negative cells), lymphoid cells (combined CD19 + and CD3 + cells), and myeloid cells (combined F4/80 + cells and Ly6C/6G + cells). Undefined cells represent all cells that expressed neither stem cell markers nor markers of lymphoid and myeloid cells. Statistical significances between groups were calculated using student's *t*-test or ANOVA. ($p \leq 0.05$ *, <0.01 **, < 0.005 ***, < 0.001 ****). n = 6 mice were used throughout the experiment.

overall cell recovery that was reduced by 35%, 48 h after the treatment. Interestingly, the total recovery of HSPCs that were positive for SCA-1 and/or cKit markers in the bone marrow cells declined by 45% in AF-SWCNT-treated mice suggesting that the toxicity of AF-SWCNTs under these particular conditions of treatment could be relatively more on HSPCs. Proportions of various cell populations in bone marrow would however depend upon a large number of factors including the numbers of active HSPCs and their proliferation, activity of supporting stromal cells, availability of growth and differentiation promoting cytokines, migration of different cell populations in and out of bone marrow etc. For this reason, it is difficult to conclude that a relatively greater decline in HSPCs in bone marrows from AF-SWCNT-treated mice was due to greater cytotoxicity of AF-SWCNTs towards HSPCs. It was therefore necessary to study the direct *in vitro* effect of AF-SWCNTs on the proliferation and differentiation of HSPCs in culture conditions.

In vitro uptake of AF-SWCNTs by HSPCs was not selective and all cells were labeled with FAF-SWCNTs. Further examination of sorted FAF-SWCNT$^+$Sca1$^+$cKit$^+$ cells by confocal microscopy indicated that FAF-SWCNTs were clearly localized in the cytoplasm, though the nuclear shadow also suggested that the particles did not traverse the nuclear membrane with the same efficiency. AF-SWCNT-treated cells started dying in culture and double labeling with Annexin-V and 7AAD suggested that the killing induced by AF-SWCNTs was through necrotic mechanism since the proportion of annexin-V$^+$7AAD$^-$ cells did not increase in AF-SWCNT-treated cultures whereas the proportion of 7AAD positive cell increased significantly. Cell cycle analysis showed that S-phase of the cell cycle was significantly reduced in AF-SWCNT treated cells. A substantial and seemingly nonselective increase was also seen in the generation of reactive oxygen species (ROS) and Caspase 3/7 enzymes in cells treated with AF-SWCNTs. ROS is one of the very first responses that follow cell abuse and can result from the damage of cell and mitochondrial membranes (Yirong, 2020). ROS production mediates the oxidative damage and further activates the Caspase enzymes that play a crucial role in the cell death pathways (Shi, 2002; Huang et al., 2011). In RT-PCR experiments, augmented expression of Caspase 3 and 9 genes was clearly seen in cells treated with AF-SWCNTs. Overall, these results point to an across the board toxic effect of AF-SWCNTs on bone marrow HSPCs.

Next set of experiments were to examine the process of ontogenesis and generation of immune cells in cultures of HSPCs. As such, bone marrow cells cultured alone quickly dwindle and die. However, addition of a cocktail of growth and differentiation promoting cytokines protects the cells and a proliferation and differentiation response can be seen *in vitro* (Metcalf, 2008; Tani-ichi et al., 2013). We use a commercially available cocktail of seven cytokines and its addition in the culture medium resulted in cell proliferation and differentiation. In eight days of culture with cytokines, cell number increased by 2.5-fold. Importantly, at the end of 8 days of culture, 62% of the cells in cytokine treated cultures were lymphoid or myeloid where none were there in the beginning of the culture. We detected the generation of few T cells also in our culture system, which would generally not be expected as T cells require thymic environment to differentiate. However, generation of T cells in bone marrow cultures has been reported before under some conditions (Freedman et al., 1996; Lehar and Bevan, 2002; Schmitt and Zúñiga-Pflücker, 2002).

Addition of AF-SWCNTs along with cytokine cocktail caused a severe decline in cell recoveries in 8 days cultures. However, there was no real decline in absolute recovery of cells and it remained the same as in the beginning of the culture. These results indicate that the cytotoxic effect of AF-SWCNTs on HSPCs was relatively lesser if cytokines were present in the culture. While the absolute cell recovery in AF-SWCNT and cytokine treated cells was only 40% of the cultures with cytokines alone, significant proliferation and differentiation seems to have proceeded along with continued cell killing activities since 53% of the cells at the end of 8 days of treatment with cytokines in presence of AF-SWCNTs were lymphoid or myeloid. It is also interesting to note that the relative proportions of lymphoid cells as well as HSPCs decreased in cells cultured with cytokines and AF-SWCNTs, as compared to cultures where only cytokines were added. Proportions of myeloid cells remained the same and proportion of cells with undefined phenotype actually increased. Hematopoietic stem cells are known to be either balanced (differentiate into equal proportion of myeloid and lymphoid cells), myeloid biased (generate few lymphoid cells) or lymphoid biased (generate few myeloid cells). Each of these types has a distinct epigenetically fixed differentiation program and their relative preponderance may change with age and regulated by cytokine milieu (Liu et al., 2009; Kong, 2018). It is possible that in the presence of AF-SWCNT differentiation of selected subpopulations of HSPCs may be promoted or suppressed. This proposition however would need to be further examined.

5. Conclusions

In summary, we found that AF-SWCNTs were strongly toxic to bone marrow cells *in vivo* as well as *in vitro* but this toxicity is significantly reduced when cells were simultaneously exposed to growth and differentiation inducing cytokines. In cultures of HSPCs with cytokine cocktail, differentiation into lymphoid and myeloid cells continued even in presence of AF-SWCNTs, albeit at lower rates.

Funding

This work was supported by Department of Science and Technology, Government of India, Nano-sciences Mission grant number SR/NM/NS-1219 and JC Bose award to RKS. MBM received fellowship support from the South Asian University.

CRediT authorship contribution statement

Md. Babu Mia: Conceptualization, Data curation, Formal analysis, Investigation, Methodology, Writing - original draft. **Rajiv K. Saxena:** Conceptualization, Formal analysis, Funding acquisition, Project administration, Resources, Software, Supervision, Validation, Visualization, Writing - review & editing.

Declaration of Competing Interest

The authors declare that they have no known competing financial interests or personal relationships that could have appeared to influence the work reported in this paper.

Appendix A. Supplementary data

Supplementary data to this article can be found online at https://doi.org/10.1016/j.crtox.2021.02.003.

References

Abu Gazia, Maha, El-Magd, Mohammed Abu, 2019. Effect of pristine and functionalized multiwalled carbon nanotubes on rat renal cortex. Acta Histochem. 121 (2), 207–217. https://doi.org/10.1016/j.acthis.2018.12.005.

Adjei, Isaac M., Sharma, Blanka, Peetla, Chiranjeevi, Labhasetwar, Vinod, 2016. Inhibition of bone loss with surface-modulated, drug-loaded nanoparticles in an intraosseous model of prostate cancer. J. Control. Release 232, 83–92. https://doi.org/10.1016/j.jconrel.2016.04.019.

Ahmadi, Homa, Ramezani, Mohammad, Yazdian-Robati, Rezvan, Behnam, Behzad, Razavi Azarkhiavi, Kamal, Hashem Nia, Azadeh, Mokhtarzadeh, Ahad, Matbou Riahi, Maryam, Razavi, Bibi Marjan, Abnous, Khalil, 2017. Acute toxicity of functionalized single wall carbon nanotubes: a biochemical, histopathologic and proteomics approach. Chem. Biol. Interact. 275, 196–209. https://doi.org/10.1016/j.cbi.2017.08.004.

Akashi, Koichi, Kondo, Motonari, Weissman, Irving L, 1998. Role of interleukin-7 in T-cell development from hematopoietic stem cells. Immunol. Rev. 165 (1), 13–28. https://doi.org/10.1111/j.1600-065X.1998.tb01226.x.

Alam, A., et al., Interactions of polydispersed single-walled carbon nanotubes with T cells resulting in downregulation of allogeneic CTL responses in vitro and in vivo. Nanotoxicology, 2013. 7(8): p. 1351-1360.

Alam, Anwar, Puri, Niti, Saxena, Rajiv K., 2016. Uptake of poly-dispersed single-walled carbon nanotubes and decline of functions in mouse NK cells undergoing activation. J. Immunotoxicol. 13 (5), 758–765. https://doi.org/10.1080/1547691X.2016.1191562.

Becher, B., Tugues, S., Greter, M., 2016. GM-CSF: from growth factor to central mediator of tissue inflammation. Immunity 45 (5), 963–973. https://doi.org/10.1016/j.immuni.2016.10.026.

Bernad, A., Kopf, M., Kulbacki, R., Weich, N., Koehler, G., Gutierrez-Ramos, J.C., 1994. Interleukin-6 is required in vivo for the regulation of stem cells and committed progenitors of the hematopoietic system. Immunity 1 (9), 725–731. https://doi.org/10.1016/S1074-7613(94)80014-6.

Broudy, V.C., 1997. Stem cell factor and hematopoiesis. Blood J. Am. Soc. Hematol. 90 (4), 1345–1364.

Canu, I.G. et al, 2020. State of knowledge on the occupational exposure to carbon nanotubes. Int. J. Hyg. Environ. Health 225, 113472.

Chen, J., Yan, L., 2017. Recent advances in carbon nanotube-polymer composites. Adv. Mater. 6 (6), 129.

del Carmen Rodríguez, M.a., A. Bernad, and M. Aracil, Interleukin-6 deficiency affects bone marrow stromal precursors, resulting in defective hematopoietic support. Blood, 2004. 103(9): p. 3349-3354.

Dutt, T.S., M.B. Mia, and R.K. Saxena, Elevated internalization and cytotoxicity of polydispersed single-walled carbon nanotubes in activated B cells can be basis for preferential depletion of activated B cells in vivo. Nanotoxicology, 2019. 13(6): p. 849-860.

Flores, Alyssa M., Hosseini-Nassab, Niloufar, Jarr, Kai-Uwe, Ye, Jianqin, Zhu, Xingjun, Wirka, Robert, Koh, Ai Leen, Tsantilas, Pavlos, Wang, Ying, Nanda, Vivek, Kojima, Yoko, Zeng, Yitian, Lotfi, Mozhgan, Sinclair, Robert, Weissman, Irving L., Ingelsson, Erik, Smith, Bryan Ronain, Leeper, Nicholas J., 2020. Pro-efferocytic nanoparticles are specifically taken up by lesional macrophages and prevent atherosclerosis. Nat. Nanotechnol. 15 (2), 154–161. https://doi.org/10.1038/s41565-019-0619-3.

Freedman, Andrew R., Zhu, Haihong, Levine, James D., Kalams, Spyros, Scadden, David T., 1996. Generation of human T lymphocytes from bone marrow CD34+ cells in vitro. Nat. Med. 2 (1), 46–51. https://doi.org/10.1038/nm0196-46.

Gangrade, Ankit, Mandal, Biman B., 2019. Injectable carbon nanotube impregnated silk based multifunctional hydrogel for localized targeted and on-demand anticancer drug delivery. ACS Biomater. Sci. Eng. 5 (5), 2365–2381. https://doi.org/10.1021/acsbiomaterials.9b00416.s001.

Huang, T.-C., J.-F. Lee, and J.-Y. Chen, Pardaxin, an antimicrobial peptide, triggers caspase-dependent and ROS-mediated apoptosis in HT-1080 cells. Marine drugs, 2011. 9(10): p. 1995-2009.

Iijima, Sumio, 1991. Helical microtubules of graphitic carbon. Nature 354 (6348), 56–58. https://doi.org/10.1038/354056a0.

Jiang, Tao, Yu, Xiaohua, Carbone, Erica J., Nelson, Clarke, Kan, Ho Man, Lo, Kevin W.-H., 2014. Poly aspartic acid peptide-linked PLGA based nanoscale particles: Potential for bone-targeting drug delivery applications. Int. J. Pharm. 475 (1-2), 547–557. https://doi.org/10.1016/j.ijpharm.2014.08.067.

Kobayashi, N., H. Izumi, and Y. Morimoto, Review of toxicity studies of carbon nanotubes. Journal of occupational health, 2017: p. 17-0089-RA.

Kong, Y., et al., Lymphoid biased hematopoietic stem cells acquire a myeloid pattern of gene expression with age. 2018, Am Assoc Immnol.

Kumari, M., S. Sachar, and R.K. Saxena, Loss of proliferation and antigen presentation activity following internalization of polydispersed carbon nanotubes by primary lung epithelial cells. PloS one, 2012. 7(2): p. e31890.

Lehar, Sophie M, Bevan, Michael J, 2002. T cell Development in culture. Immunity 17 (6), 689–692. https://doi.org/10.1016/S1074-7613(02)00477-6.

Liu, Z. et al, 2011. Carbon materials for drug delivery & cancer therapy. Mater. Today 14 (7–8), 316–323.

Liu, Z., Davis, C., Cai, W., He, L., Chen, X., Dai, H., 2008. Circulation and long-term fate of functionalized, biocompatible single-walled carbon nanotubes in mice probed by Raman spectroscopy. Proc. Natl. Acad. Sci. 105 (5), 1410–1415. https://doi.org/10.1073/pnas.0707654105.

Liu, Zhuang, Tabakman, Scott, Welsher, Kevin, Dai, Hongjie, 2009. Carbon nanotubes in biology and medicine: In vitro and in vivo detection, imaging and drug delivery. Nano Res. 2 (2), 85–120. https://doi.org/10.1007/s12274-009-9009-8.

Ma, Juan, Li, Ruibin, Liu, Yin, Qu, Guangbo, Liu, Jing, Guo, Wenli, Song, Haoyang, Li, Xinghong, Liu, Yajun, Xia, Tian, Yan, Bing, Liu, Sijin, 2017. Carbon nanotubes disrupt iron homeostasis and induce anemia of inflammation through inflammatory pathway as a secondary effect distant to their portal-of-entry. Small 13 (15), 1603830. https://doi.org/10.1002/smll.201603830.

Madani, Seyed Yazdan, Mandel, Abraham, Seifalian, Alexander M., 2013. A concise review of carbon nanotube's toxicology. Nano Rev. 4 (1), 21521. https://doi.org/10.3402/nano.v4i0.21521.

Md, B.M., Saxena, R., 2018. Phosphatidyl serine externalization in different age groups of mouse erythrocytes in response to agents that induce anemia. Hematol. Transfus. Int. J. 6 (4), 144–149.

Metcalf, D., Hematopoietic cytokines. Blood, The Journal of the American Society of Hematology, 2008. 111(2): p. 485-491.

Babu Mia, Md., Saxena, Rajiv K., 2020. Poly dispersed acid-functionalized single walled carbon nanotubes target activated T and B cells to suppress acute and chronic GVHD in mouse model. Immunol. Lett. 224, 30–37. https://doi.org/10.1016/j.imlet.2020.05.006.

Nolan, Tania, Hands, Rebecca E, Bustin, Stephen A, 2006. Quantification of mRNA using real-time RT-PCR. Nat. Protoc. 1 (3), 1559–1582. https://doi.org/10.1038/nprot.2006.236.

Oparka, Monika, Walczak, Jarosław, Malinska, Dominika, van Oppen, Lisanne M.P.E., Szczepanowska, Joanna, Koopman, Werner J.H., Wieckowski, Mariusz R., 2016. Quantifying ROS levels using CM-H 2 DCFDA and HyPer. Methods 109, 3–11. https://doi.org/10.1016/j.ymeth.2016.06.008.

Orkin, S.H., Zon, L.I., 2008. Hematopoiesis: an evolving paradigm for stem cell biology. Cell 132 (4), 631–644. https://doi.org/10.1016/j.cell.2008.01.025.

Prato, Maurizio, Kostarelos, Kostas, Bianco, Alberto, 2008. Functionalized carbon nanotubes in drug design and discovery. Acc. Chem. Res. 41 (1), 60–68. https://doi.org/10.1021/ar700089b.

Redza-Dutordoir, Maureen, Averill-Bates, Diana A., 2016. Activation of apoptosis signalling pathways by reactive oxygen species. Biochim. Biophys. Acta (BBA) – Mol. Cell Res. 1863 (12), 2977–2992. https://doi.org/10.1016/j.bbamcr.2016.09.012.

Rizvi, Zaigham Abbas, Puri, Niti, Saxena, Rajiv K., 2015. Lipid antigen presentation through CD1d pathway in mouse lung epithelial cells, macrophages and dendritic cells and its suppression by poly-dispersed single-walled carbon nanotubes. Toxicol. In Vitro 29 (6), 1275–1282. https://doi.org/10.1016/j.tiv.2014.10.022.

Sachar, S. and R.K. Saxena, Cytotoxic effect of poly-dispersed single walled carbon nanotubes on erythrocytes in vitro and in vivo. PLoS One, 2011. 6(7): p. e22032.

Saxena, R.K., et al., Enhanced in vitro and in vivo toxicity of poly-dispersed acid-functionalized single-wall carbon nanotubes. Nanotoxicology, 2007. 1(4): p. 291-300.

Schipper, Meike L., Nakayama-Ratchford, Nozomi, Davis, Corrine R., Kam, Nadine Wong Shi, Chu, Pauline, Liu, Zhuang, Sun, Xiaoming, Dai, Hongjie, Gambhir, Sanjiv S., 2008. A pilot toxicology study of single-walled carbon nanotubes in a small sample of mice. Nat. Nanotechnol. 3 (4), 216–221. https://doi.org/10.1038/nnano.2008.68.

Schmitt, Thomas M., Zúñiga-Pflücker, Juan Carlos, 2002. Induction of T Cell development from hematopoietic progenitor cells by delta-like-1 in vitro. Immunity 17 (6), 749–756. https://doi.org/10.1016/S1074-7613(02)00474-0.

Shi, Yigong, 2002. Mechanisms of caspase activation and inhibition during apoptosis. Mol. Cell 9 (3), 459–470. https://doi.org/10.1016/S1097-2765(02)00482-3.

Singh, A.P., Mia, M.B., Saxena, R.K., 2020. Acid-functionalized single-walled carbon nanotubes alter epithelial tight junctions and enhance paracellular permeability. J. Biosci. 45 (1), 1–12.

Stevens, Tina, Saxena, Rajiv, Ian Gilmour, M., 2006. In: Particle Toxicology. Informa Healthcare, pp. 245–257. https://doi.org/10.1201/9781420003147.ch13.

Swami, A., et al., Engineered nanomedicine for myeloma and bone microenvironment targeting. Proceedings of the National Academy of Sciences, 2014. 111(28): p. 10287-10292.

Tani-ichi, S., Shimba, A., Wagatsuma, K., Miyachi, H., Kitano, S., Imai, K., Hara, T., Ikuta, K., 2013. Interleukin-7 receptor controls development and maturation of late stages of thymocyte subpopulations. Proc. Natl. Acad. Sci. 110 (2), 612–617. https://doi.org/10.1073/pnas.1219242110.

Wilkinson, A.C., Igarashi, K.J., Nakauchi, H., 2020. Haematopoietic stem cell self-renewal in vivo and ex vivo. Nat. Rev. Genet. 21 (9), 541–554. https://doi.org/10.1038/s41576-020-0241-0.

Wu, Wei, Li, Rutian, Bian, Xiaochen, Zhu, Zhenshu, Ding, Dan, Li, Xiaolin, Jia, Zhijun, Jiang, Xiqun, Hu, Yiqiao, 2009. Covalently combining carbon nanotubes with anticancer agent: preparation and antitumor activity. ACS Nano 3 (9), 2740–2750. https://doi.org/10.1021/nn9005686.

Xia, X., Li, L., Choi, Y.S., 1992. Human recombinant IL-3 is a growth factor for normal B cells. J. Immunol. 148 (2), 491–497.

Yamamoto, R., Morita, Y., Ooehara, J., Hamanaka, S., Onodera, M., Rudolph, K., Ema, H., Nakauchi, H., 2013. Clonal analysis unveils self-renewing lineage-restricted progenitors generated directly from hematopoietic stem cells. Cell 154 (5), 1112–1126. https://doi.org/10.1016/j.cell.2013.08.007.

Yirong, C. et al, 2020. DEHP induces neutrophil extracellular traps formation and apoptosis in carp isolated from carp blood via promotion of ROS burst and autophagy. Environ. Pollut. 262, 114295.

Zhang, Minfang, Xu, Ying, Yang, Mei, Yudasaka, Masako, Okazaki, Toshiya, 2020. Clearance of single-wall carbon nanotubes from the mouse lung: a quantitative evaluation. Nanoscale Adv. 2 (4), 1551–1559. https://doi.org/10.1039/D0NA00040J.